

This discussion paper is/has been under review for the journal Hydrology and Earth System Sciences (HESS). Please refer to the corresponding final paper in HESS if available.

Impact of controlled changes in grain size and pore space characteristics on the hydraulic conductivity and spectral induced polarization response of “proxies” of saturated alluvial sediments

K. Koch¹, A. Kemna², J. Irving^{1,3}, and K. Holliger¹

¹Institute of Geophysics, University of Lausanne, 1015 Lausanne, Switzerland

²Department of Geodynamics and Geophysics, University of Bonn, 53115 Bonn, Germany

³School of Engineering, University of Guelph, Guelph, Ontario, N1G 2W1, Canada

Received: 12 August 2010 – Accepted: 19 August 2010 – Published: 24 August 2010

Correspondence to: K. Koch (kristof.koch@unil.ch)

Published by Copernicus Publications on behalf of the European Geosciences Union.

6057

Abstract

Understanding the influence of pore space characteristics on the hydraulic conductivity and spectral induced polarization (SIP) response is critical for establishing relationships between the electrical and hydrological properties of surficial unconsolidated sedimentary deposits, which host the bulk of the world's readily accessible ground-water resources. Here, we present the results of laboratory SIP measurements on industrial-grade, saturated quartz samples with granulometric characteristics ranging from fine sand to fine gravel, which can be regarded as proxies for widespread alluvial deposits. We altered the pore space characteristics by changing (i) the grain size spectra, (ii) the degree of compaction, and (iii) the level of sorting. We then examined how these changes affect the SIP response, the hydraulic conductivity, and the specific surface area of the considered samples. In general, the results indicate a clear connection between the SIP response and the granulometric as well as pore space characteristics. In particular, we observe a systematic correlation between the hydraulic conductivity and the relaxation time of the Cole-Cole model describing the observed SIP effect for the entire range of considered grain sizes. The results do, however, also indicate that the detailed nature of these relations depends strongly on variations in the pore space characteristics, such as, for example, the degree of compaction. The results of this study underline the complexity of the origin of the SIP signal as well as the difficulty to relate it to a single structural factor of a studied sample, and hence raise some fundamental questions with regard to the practical use of SIP measurements as site- and/or sample-independent predictors of the hydraulic conductivity.

1 Introduction

Knowledge of the distribution of the hydraulic conductivity within an aquifer is a key prerequisite for reliable predictions of groundwater flow and contaminant transport. This information is in turn critical for the effective protection, remediation, and sustainable

6058

management of the increasingly scarce and fragile groundwater resources in densely populated and/or highly industrialized regions throughout the world. To this end, geophysical constraints with regard to aquifer structure and the distribution of hydraulic parameters are considered to be particularly valuable. The primary reasons for this are that geophysical methods are inexpensive and non-invasive in nature and that they have the potential to bridge an inherent gap which exists in terms of spatial resolution and coverage between traditional hydrogeological methods such as core analyses and tracer or pumping tests (e.g., Rubin and Hubbard, 2005; Koch et al., 2009).

Although standard geophysical techniques cannot in general provide any direct information on the hydraulic conductivity in the subsurface, there are a number of more specialized approaches that exhibit a more-or-less direct sensitivity to this important parameter. Together with nuclear magnetic resonance techniques and the interpretation of seismic observations in a poro-elastic context, induced polarization (IP) measurements in general and spectral induced polarization (SIP) measurements in particular arguably represent the most promising approaches (e.g., Slater, 2007; Holliger, 2008). Indeed, one of the major goals of advancing our knowledge about the electrical characteristics of porous media is the possibility of linking parameters derived from the corresponding IP and/or SIP responses to hydrologically relevant parameters (e.g., Lesmes and Friedman, 2005).

The IP-type polarization of non-metallic minerals is generally referred to as interface or membrane polarization (Marshall and Madden, 1959; Vinegar and Waxman, 1984) and takes place in the lower frequency range up to the Maxwell-Wagner effect (Maxwell, 1892; Wagner, 1914; Chen and Or, 2006). In the absence of metallic conductors, such as ore minerals or graphite, SIP phenomena are commonly associated with polarization effects related to a polarized electrical double layer (EDL). The EDL schematically describes the organization of ionic charges at the interface between solid and fluid and was first introduced by Helmholtz in the middle of the 19th century. The inner layer is given by the typically negatively charged mineral surface attracting positively charged ions contained in the pore fluid to form the supposedly firmly attached

6059

Stern layer (Stern, 1924). Beyond the Stern layer, positively charged ions continue to be attracted by the negatively charged mineral surface, but at the same time are repelled by each other and the Stern layer. The resulting dynamic equilibrium is referred to as the diffuse layer and represents the transition zone towards the outer limit of the EDL, where ions are in equilibrium with the solution and distributed in a random manner. The EDL provides the conceptual background for the electrochemical processes considered to be responsible for much of the observed SIP response, as documented, for example, by the recent study of Leroy et al. (2008).

Much of today's conceptual understanding of the origin of the SIP response is based on the work by Schwarz (1962) and his interpretation of the SIP effect as a result of the redistribution of counter-ions surrounding spherical particles in suspension. The only geometric factor involved in the model is the size of the sphere. Translating this geometrically simple analytical model to texturally complex porous media is not evident. Titov et al. (2004) attempted to provide a visualization of the two basic conceptual views on the origin of the SIP effect in porous media linking it either to the grain-size distribution or to the pore-size distribution. A number of studies have attempted to gain further insight into these matters by attributing the polarization to the EDL surrounding individual grains (e.g., Lesmes and Morgan, 2001) and to excesses and deficiencies in ion concentrations along pore throats (e.g., Titov et al., 2002). In virtually all of these studies, the relaxation time or relaxation frequency has been theoretically related to a certain length scale representing either the grain radius (Schwarz, 1962) or a pore length scale (Kormiltsev, 1963).

A good phenomenological description of the observed SIP responses was found to be provided by Cole-Cole-type models (e.g., Vanhala, 1997) and good correlations for different sets of materials, between hydraulic conductivity and the Cole-Cole time constant were found (e.g., Binley et al., 2005; Kemna et al., 2005; Zisser et al., 2010). Although a clear link between hydrological properties and IP/SIP parameters has been empirically documented by various studies (e.g., Börner et al., 1996; Slater and Lesmes, 2002; Kemna et al., 2004; Binley et al., 2005; Hördt et al., 2007; Slater,

6060

2007), the detailed nature and origin of such linkages remain enigmatic. For example, the mineralogical and granulometric range of unconsolidated clastic sediments for which SIP effects can be reliably detected and related to the governing hydraulic properties is as of yet largely unexplored. In particular, it is not clear to what extent SIP methods are applicable to weakly polarizeable, clay-poor alluvial deposits, which characterize some of the world's most important surficial aquifers. It is also not yet clear how basic changes in the pore space and/or grain size characteristics affect the SIP response and its relation to the hydraulic conductivity.

In this paper, we address some of these questions through SIP measurements on saturated industrial-grade granular quartz samples with effective grain sizes ranging from fine sand to fine gravel, which in many ways can be regarded as first-order proxies for surficial alluvial deposits. The pore space and grain size characteristics of the original samples are modified through compaction and sieving, while the chemistry of the saturating pore fluid is kept constant for comparison of the impact of structural changes on the SIP response. In the following, we first describe the experimental setup used in this study, the granulometric properties of our samples, and the basic methodology of the data analysis. We then proceed to explore the relation between the corresponding SIP responses and the hydraulic properties.

2 Experimental procedure and data analysis

We have performed laboratory-based measurements on water-saturated industrial-grade granular quartz samples over a very broad range of average grain diameters from fine sand to fine gravel (Table 1, Fig. 1). For these measurements, the pore space characteristics of the samples were modified by varying (i) the grain size, (ii) the degree of compaction, and (iii) the degree of sorting. We then examined how these changes affected the hydraulic conductivity, specific surface area, and the SIP response of the considered samples. Compaction was achieved through handheld multidirectional vibration. The shaking was continued until the sample volume stabilized at 90% of

6061

its original volume. Sieving the sands F36 and WQ1 provided extremely well sorted samples of grain sizes: 0.09–0.125 mm, 0.125–0.18 mm, 0.18–0.25 mm, 0.25–0.5 mm, 0.5–0.71 mm, and 0.71–1.0 mm.

Measurements of the hydraulic conductivity were made using the constant head method. Specific surface area analysis was undertaken through the use of laser diffractometry. The SIP measurements were conducted over a frequency range from 1 mHz to 45 kHz and electrical conductivities of $\sim 60 \mu\text{S}/\text{cm}$ and $\sim 300 \mu\text{S}/\text{cm}$ were considered for the saturating pore fluids. In this context, it is important to note that in general the signal-to-noise ratio of the observed phase spectra improved significantly with decreasing electrical conductivity of the pore fluid. This is due to the fact that the SIP phase spectrum essentially corresponds to the ratio of the complex and real parts of the electrical conductivity and thus reflects the increasing relative importance of the complex surface conductivity processes taking place in the EDL at low conductivities of the saturating pore fluid. The SIP measurements were carried out using the highly sensitive impedance spectrometer for weakly polarizeable media developed by Zimmermann et al. (2008). The cylinder holding the sample has a length of 30 cm and a diameter of 6 cm. The current electrodes, consisting of porous bronze plates with an effective pore diameter of $15 \mu\text{m}$, form the upper and lower boundaries of the sample volume. The potential electrodes are rings of silver wire fixed in grooves at $1/3$ and $2/3$ of the sample holder's length thus resulting in a constant, Wenner-type spacing of 10 cm between the individual electrodes. The sample's response to the applied current is recorded and provides information about the real and imaginary parts of the electrical resistivity.

To analyze the measured complex resistivity data, we first fit them using the so-called Cole-Cole model (Cole and Cole, 1941) given by

$$\rho(\omega) = \rho_0 \left[1 - m \left(1 - \frac{1}{1 + (i\omega\tau)^c} \right) \right], \quad (1)$$

where ω denotes angular frequency, ρ_0 the low-frequency asymptote, or direct-current value, of the electrical resistivity $\rho(\omega)$, m the chargeability, c the Cole-Cole exponent, τ the time constant or relaxation time, and $i = \sqrt{-1}$. The chargeability m describes the

6062

magnitude of the polarization effect, the Cole-Cole exponent c determines the width of the peak of the phase curve described by Eq. (1), and the time constant τ is related to the location of this peak in the frequency band (e.g., Lesmes and Friedman, 2005; Cosenza et al., 2009). The exponent c typically takes values in the range from
5 ~ 0.2 to ~ 0.7 , with smaller values being associated with broader resonance peaks. In a number of previous laboratory-based SIP studies, relaxation time has been found to exhibit a more-or-less clear correlation with the hydraulic conductivity (e.g., Pape and Vogelsang, 1996; Kemna et al., 2005; Binley et al., 2005). In view of the pronounced
10 non-linearity and small number of parameters of the Cole-Cole model, we decided to use a Bayesian Markov-chain-Monte-Carlo inversion approach for estimating the underlying parameters from the measured SIP data (e.g., Mosegaard and Tarantola, 1995; Chen et al., 2008). We considered uniform prior distributions for all parameters except for the low-frequency asymptote of the resistivity ρ_0 , which we set to the resistivity value observed at the lowest measurement frequency of 1 mHz. Experimenting
15 with the width of these prior distributions, we found that it had essentially no influence on the final result and only a relatively minor influence on the speed of convergence, which points to the inherent robustness of the inversion procedure.

Figure 2 shows a representative log-log plot of the observed phase as a function of the frequency from one of our SIP measurements. The corresponding saturated
20 quartz sand sample was measured three times up and down the considered frequency range and clearly displays the resonance or relaxation effect described through the Cole-Cole model given by Eq. (1). For the considered data set, the resonance peak is located at ~ 1 Hz. At ~ 50 Hz the graph shows some erratic noise, which is most likely related to the local power supply. For comparison, we also show the corresponding
25 measurements for the saturating pore fluid only, which in this case was water with an electrical conductivity of $\sim 60 \mu\text{S}/\text{cm}$.

Overall, we found that data quality is a significant issue for SIP measurements on weakly polarizable samples. In particular, we have noticed that our SIP measurements were adversely affected in the lower frequency range between ~ 0.001 and 0.01 Hz.

6063

Although similar observations have been made by other researchers (Jougnot, personal communication, 2009; Okay, personal communication, 2009), the causes of these noise problems remain enigmatic. As a consequence, SIP measurements on the more coarse-grained samples, whose relaxation peaks are expected to be located
5 at the lower end of the considered frequency range, must probably be regarded as representing the limits of current measurement capabilities. In this context, it is, however, important to note that due to the use of multiple repeated measurements over the entire frequency range and variable electrical conductivities of the saturating pore fluid, meaningful quantitative interpretations were, unless explicitly mentioned other-
10 wise, possible for most of our samples.

3 Results

3.1 Hydraulic characterization

Figure 3 shows a semi-log plot of the saturated hydraulic conductivity versus porosity for the samples considered in this study. The samples are distinguished in terms of
15 being compacted, non-compacted, sieved, and non-sieved. As expected, we observe that the compaction of a sample generally results in a reduced hydraulic conductivity and porosity due to smaller pore diameters. Changing of the grain size distributions through the use of sieved fractions, on the other hand, shows a tendency towards greater porosity values for comparable values of the hydraulic conductivities. At similar
20 porosity, well-sorted samples tend to drain less efficiently than their more heterogeneous counterparts, and in other words need more pore space to conduct the same amount of water. It is assumed that pore size distribution is more homogeneous in well-sorted samples, and discrepancies between smallest and biggest pore sizes are smaller than with materials of broad grain size distributions. The above finding is consistent with the fact that a squared increase of the pore surface area, which governs
25 frictional properties, is opposed by a cubic gain in pore volume, which governs the

6064

transport volume. Meaning that one pore with the same volume as two smaller pores combined imposes less friction on the water flux and hence transports more water in the same time. Although this statement seems to be largely self-evident and a principal factor in the formation of preferential, channelized flow patterns, this effect is rarely considered in current hydrological research (e.g., Hillel, 2004).

Figure 4 shows a semi-log plot of the saturated hydraulic conductivity versus the specific surface area. The specific surface area was evaluated with a Beckman Coulter LS™ 13320 Laser Diffraction Particle Size Analyzer. The method is applicable for non-compacted samples with grain diameters smaller than 2 mm and hence the total amount of measureable samples is somewhat limited. Nevertheless, the corresponding results demonstrate that well sorted samples show a much stronger and clearer correlation between hydraulic conductivity and specific surface area compared to their more poorly sorted, more heterogeneous counterparts. Overall, we see that for comparable surface areas, well sorted samples are characterized by higher hydraulic conductivity than most of the more poorly sorted samples. Keeping in mind the above mentioned basic relationship of surface to volume, this discrepancy between sieved and non-sieved sands should be entirely related to the heterogeneity of the samples' pore structure. As a consequence, the discrepancy between the maximum value of the specific surface area for a certain value of the hydraulic conductivity and the actually observed value for a given sample should provide us with a parameter related to the actual width of a samples pore size distribution. This parameter is related to the dynamic storage and hydraulic transport behavior of a material and might be of use in hydrological modeling. In the considered case, the maximum values case are given by the results for the well sorted samples, but could also be inferred through theoretical considerations.

3.2 SIP measurements

Figure 5 shows a log-log plot of the saturated hydraulic conductivity versus the estimated relaxation time τ obtained by inverting the measured SIP data based on the

6065

Cole-Cole model given by Eq. (1). Only compacted samples are considered and the results were separated in terms of being sieved or non-sieved before least-squares fitting. We see that non-sieved samples exhibit a systematic relation between the hydraulic conductivity K and the relaxation time τ of the form $\log K = a + b \log \tau$. The correlation between K and τ is much stronger for the non-sieved samples than for the sieved samples, which we attribute to the generally relatively poor quality of the SIP measurements for the latter. This finding, which has been corroborated through repeated measurements, is enigmatic when interpreting the SIP-response based on the simple sphere model from Schwarz (1962). When considering the grain diameter to be one of the most decisive parameters we would expect to see a trend towards sharper, more clear, relaxation peaks, along with increasing granulometric homogeneity of the samples, which indirectly should result in a more clear K - τ correlation for better sorted sand.

Figure 6 shows a log-log plot of the saturated hydraulic conductivity versus the estimated Cole-Cole relaxation time, where we have now separated the samples with regard to being either compacted or non-compacted. With regard to time constant τ , the overall effect of compaction thus seems to be a shift towards smaller time constants, associated with smaller length scales of the underlying polarization process (Schwarz, 1962; Kormiltsev, 1963). The primary effect of compaction is the reduction of the porosity but likewise it results in increasing a sample's specific surface area: for example, decreasing the pore space between uniform spheres by 10% through compaction results in an increase of the specific surface area of almost 17%. This demonstrates that together with the well known sensitivity of the SIP response to changes in grain size (e.g., Schwartz, 1962; Leroy et al., 2008; Revil and Florsch, 2010), the specific surface area also seems to be a good indicator of the size of the polarization cells sensed by the inferred relaxation processes (e.g., Kormiltsev, 1963; Börner and Schön, 1991)

Finally, Fig. 7 compares the observed K values with inferred ones based on common granulometric models (Hazen, 1892; Beyer, 1964) with the τ values of the corre-

6066

sponding samples. Interestingly, we find a systematically stronger correlation for the measured K -values compared to the K -values inferred from empirical relations based on granulometric criteria. These findings corroborate the above interpretation and are consistent with the original findings of Kozeny (1927) and Carman (1938, 1956) in that the specific surface area of a porous material is in general the determining parameter for its permeability.

Following Reppert and Morgan (2001), Scott (2006), and Revil and Florsch (2010), the impact of the pore width on the recorded SIP response can be considered of secondary importance. This is primarily due to the comparatively large sizes of the pore throats of both the non-compacted and the compacted samples considered in this study, which in turn points to the generally subordinate contribution of pore throat and membrane effects to the observed SIP response for unconsolidated sandy sediments in the frequency range below the Maxwell-Wagner effect. At the same time, the observed impact on a samples' SIP-signature related to the transformation of pore space through compaction clearly indicates that individual structural aspects like grain size or surface roughness (e.g., Leroy et al., 2008) are not the only parameters determining SIP response. Compaction changes the specific surface area, which in turn is expected to find its distinct expression in corresponding changes of the formation factor. As a consequence, the recently proposed theoretical model from Revil and Florsch (2010), in which the formation factor plays an essential role, seems to be indirectly supported by our findings. In detail, however, the link between the formation factor and the SIP response of granular sandy media is as of yet largely unexplored and, in our view, represents pertinent a topic for future research in this domain.

4 Conclusions

The goal of this study was to improve our understanding of the polarization processes through experimental control of different pore space characteristics in laboratory measurements. It can safely be stated that our results show a clear relation of the SIP re-

6067

sponse with the hydraulic conductivity, demonstrate the variability of this relation in response to changes in pore size and grain size characteristics, and hence demonstrate potential of SIP-based methods for remote-sensing-type first-order hydraulic characterizations of the shallow subsurface. In agreement with previous findings, the results of our measurements indicate a power-law-type correlation between the inferred Cole-Cole relaxation time and hydraulic conductivity for the considered broad range of saturated sand samples. Changes in compaction and sorting of the samples resulted in a certain shift in the SIP response but did not fundamentally alter this overall picture. With regard to an improved understanding of the underlying physical properties, the strong interdependencies between grain size distribution and pore characteristics complicate the inference of the origin of the corresponding SIP effect. Yet, increasing the degree of compaction while leaving the grain size distribution unchanged showed a systematic effect on the SIP response towards smaller relaxation times, which in turn are associated with lower degrees of heterogeneity in the probed material. The phenomenological approach of relating values of the relaxation time to a change in the size of heterogeneities in the sampled material showed for both changes in grain size and pore size of our samples, while the change of pore size through compaction also effects the ratio pore interface versus porosity. Due to this interlink of specific surface area with compaction and pore width, multiple explanations are possible and hence fundamental question regarding the interdependencies of the polarization spectra and pore width remains as of yet unresolved.

Acknowledgements. This research has been funded by a grant from the Swiss National Science Foundation. We greatly profited from collaboration with and logistical support from the Forschungszentrum Juelich, Germany. We would also like to thank Quarzwerke Frechen for providing the samples used for this study.

References

- Beyer, W.: Zur Bestimmung der Wasserdurchlässigkeit von Kiesen und Sanden aus der Kornverteilung, *Wasserwirtschaft – Wassertechnik (WWT)*, 165–169, 1964.
- Binley, A., Slater L., Fukes M., and Cassiani, G.: The relationship between spectral induced polarization and hydraulic properties of saturated and unsaturated sandstone, *Water Resour. Res.*, 41(12), W12417, doi:10.1029/2005WR004202, 2005.
- Börner, F. D. and Schön, J. H.: A relation between the quadrature component of electrical conductivity and the specific surface area of sedimentary rocks, *The Log Analyst*, 32, 612–613, 1991.
- Börner, F. D., Schopper, J. R., and Weller, A.: Evaluation of transport and storage properties in the soil and groundwater zone from induced polarization measurements, *Geophys. Prospect.*, 44, 583–601, 1996.
- Chen, Y. and Or, D.: Effects of Maxwell-Wagner polarization on soil complex dielectric permittivity under variable temperature and electrical conductivity, *Water Resour. Res.*, 42, W06424, doi:10.1029/2005WR004590, 2006.
- Chen, J., Kemna, A., and Hubbard, S.: A comparison between Gauss-Newton and Markov-chain Monte Carlo-based methods for inverting spectral induced-polarization data for Cole-Cole parameters, *Geophysics*, 73, F247–F259, doi:10.1190/1.2976115, 2008.
- Cole, K. S. and Cole, R. H.: Dispersion and absorption in dielectrics. I. alternating current field, *J. Chem. Phys.*, 1, 341–351, 1941.
- Cosenza, P., Ghorbani, A., Camerlynck, C., Rejiba, F., Guérin, R., and Tabbagh, A.: Effective medium theories for modelling the relationships between electromagnetic properties and hydrological variables in geomaterials: a review, *Near Surf. Geophys.*, 7, 563–578, doi:10.3997/1873-0604.2009009, 2009.
- Carman, P. C.: The determination of the specific surface of powders, *J. Soc. Chem. Ind. Trans.*, 57, 225–234, 1938.
- Carman, P. C.: *Flow of gases through porous media*, Butterworths Scientific Publications, London, 1956.
- Hazen, A.: Some physical properties of sands and gravels, with special reference to their use in filtration, 24th Annual Rep., Massachusetts State Board of Health, 34, 539–556, 1892.
- Hillel, D.: *Introduction to environmental soil physics*, Elsevier, 494 pp., 2004.
- Holliger, K.: Groundwater geophysics: from structure and porosity to permeability?, in: Over-

6069

- exploitation and contamination of shared groundwater resources, edited by: Darnault, C., Springer, 49–65, 2008.
- Hördt, A., Blaschek, R., Kemna, A., and Zisser, N.: Hydraulic conductivity estimation from induced polarisation data at the field scale – the Krauthausen case history, *J. Appl. Geophys.*, 62, 33–46, 2007.
- Kemna, A., Binley, A., and Slater, L.: Crosshole IP imaging for engineering and environmental applications, *Geophysics*, 69, 97–107, 2004.
- Kemna, A., Münch, H.-M., Titov, K., Zimmermann, E., and Vereecken, H.: Relation of SIP relaxation time of sands to salinity, grain size and hydraulic conductivity: Extended Abstracts: Near Surface 2005 – 11th European Meeting of Environmental and Engineering Geophysics, 4 pp, 2005.
- Koch, K., Wenninger, J., Uhlenbrook, S., and Bonell, M.: Joint interpretation of hydrological and geophysical data: electrical resistivity tomography results from a process hydrological research site in the Black Forest Mountains, Germany, *Hydrol. Process.*, 23(10), 1501–1513, 2009.
- Kormiltsev, V. V.: O vzbuzdenii i spade vyzvannoi polarizatsii v kapillarnoi srede (On excitation and decay of Induced Polarization in capillary medium): *Izvestia AN SSSR, Seria Geofizicheskaya (Solid Earth Physics)*, 11, 1658–1666, (in Russian), 1963.
- Kozeny, J.: *Ueber kapillare Leitung des Wassers im Boden*, Wien, Akad. Wiss., 136(2a), 271, (in German), 1927.
- Leroy, P., Revil, A., Kemna, A., Cosenza, P., and Ghorbani, A.: Complex conductivity of water-saturated packs of glass beads, *J. Colloid Interf. Sci.*, 321, 103–117, 2008.
- Lesmes, D. P. and Morgan, F. D.: Dielectric spectroscopy of sedimentary rocks, *J. Geophys. Res.*, 106, 13329–13346, 2001.
- Lesmes, D. P. and Friedman, S.: Relationships between electrical and hydrogeological properties of rocks and soils, in: *Hydrogeophysics*, edited by: Rubin, Y. and Hubbard, S., Springer, Dordrecht, The Netherlands, 129–156, 2005.
- Marshall, D. J. and Madden, T. R.: Induced polarization, a study of its causes, *Geophysics*, 24, 790–816, 1959.
- Maxwell, J. C.: *A Treatise on Electricity and Magnetism*, third ed., Oxford University Press, London, 1892.
- Mosegaard, K. and Tarantola, A.: Monte Carlo sampling of solutions to inverse problems, *J. Geophys. Res.*, 100, 12431–12447, doi:10.1029/94JB03097, 1995.

6070

- Pape, H. and Vogelsang, D.: Fractal Evaluation of Induced Polarization Logs in the KTB-Oberpfalz HB, *Geologisches Jahrbuch, Bundesanst. für Geowiss. u. Rohstoffe*, E 54, 3–27, 1996.
- Reppert, P. M. and Morgan, F. D.: Streaming potential data collection and data processing techniques, *J. Colloid Interf. Sci.*, 233, 348–355, 2001.
- Revil, A. and Florsch, N.: Determination of permeability from spectral induced polarization in granular media, *Geophys. J. Int.*, 181(3), 1480–1498, doi:10.1111/j.1365-246X.2010.04573.x, 2010.
- Rubin, Y. and Hubbard, S.: *Hydrogeophysics*, Springer, Dordrecht, The Netherlands, 523 pp., 2005.
- Scott, J. B. T.: The origin of the observed low-frequency electrical polarization in sandstones, *Geophysics*, 71, 235–238, 2006.
- Schwarz, G.: A theory of the low-frequency dispersion of colloidal particles in electrolyte solution, *J. Phys. Chem.*, 66, 2636–2642, 1962.
- Slater, L. and Lesmes, D. P.: Electrical-hydraulic relationships observed for unconsolidated sediments, *Water Resour. Res.*, 38(10), 1213, doi:10.1029/2001WR001075, 2002.
- Slater, L.: Near Surface Electrical Characterization of Hydraulic Conductivity: From Petrophysical Properties to Aquifer Geometries – A Review, *Surv. Geophys.*, 28, 169–197, 2007.
- Stern, O.: Zur Theorie der elektrolytischen Doppelschicht, *Z. Electrochem*, 30, 508, (in German), 1924.
- Titov, K., Komarov, V., Tarasov, V., and Levitski, A.: Theoretical and experimental study of time-domain induced polarization in water saturated sands, *J. Appl. Geophys.*, 50, 417–433, 2002.
- Titov, K., Kemna, A., Tarasov, A., and Vereecken, H.: Induced Polarization of Unsaturated Sands Determined through Time Domain Measurements, *Vadose Zone J.*, 3, 1160–1168, 2004.
- Vanhala, H.: Mapping oil-contaminated sand and till with the spectral induced polarization (SIP) method, *Geophys. Prosp.*, 45, 303–326, 1997.
- Vinegar, H. J. and Waxman, M. H.: Induced polarization of shaly sands, *Geophysics*, 49, 1267–1287, 1984.
- Wagner, K. W.: *Arch. Elektrotechn*, 2, 371–387, 1914.
- Zimmermann, E., Kemna, A., Berwix, J., Glaas, W., Münch, H. M., and Huisman, J. A.: A high-accuracy impedance spectrometer for measuring sediments with low polarizability, *Meas. Sci. Technol.*, 19, 105603, doi:10.1088/0957-0233/19/10/105603, 2008.
- Zisser, N., Kemna, A., and Nover, G.: Relationship between low-frequency electrical properties and hydraulic permeability of low-permeability sandstones, *Geophysics*, 75, E131–E141, 2010.

6071

6072

Table 1. Table of the original, unsieved samples and their effective and medium grain sizes d_{10} and d_{50} , respectively, and their level of sorting as defined by d_{60}/d_{10} .

	F36	F34	F32	WQ1	WQ2	WQ3	WQ4	WQ6
Aggregate class	Fine sand	Medium sand	Medium sand	Medium sand	Coarse sand	Coarse sand	Coarse sand	Fine gravel
d_{10} [mm]	0.12	0.14	0.16	0.47	0.75	1.06	1.46	2.7
d_{50} [mm]	0.17	0.21	0.23	0.62	0.99	1.35	1.84	3.41
d_{60}/d_{10}	1.50	1.57	1.50	1.38	1.40	1.31	1.31	1.33

6073

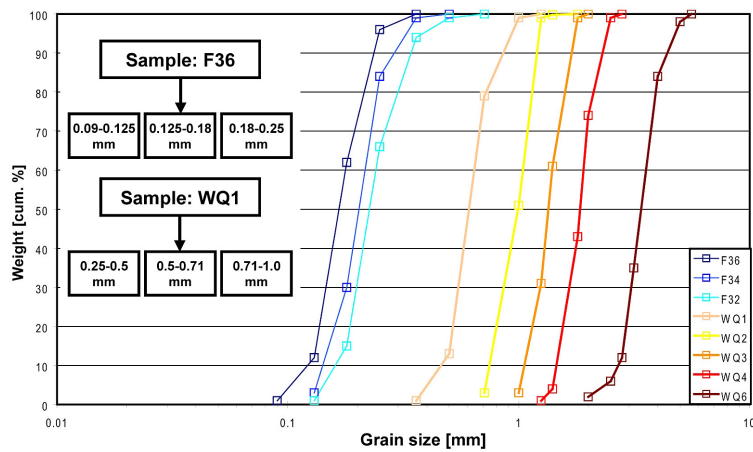


Fig. 1. Grain size distribution curves for the different samples considered in this study. Left: Six sieved fractions originating from sands F36 and WQ1. Right: Grain size distributions of unsieved industrial granular quartz samples. See also Table 1.

6074

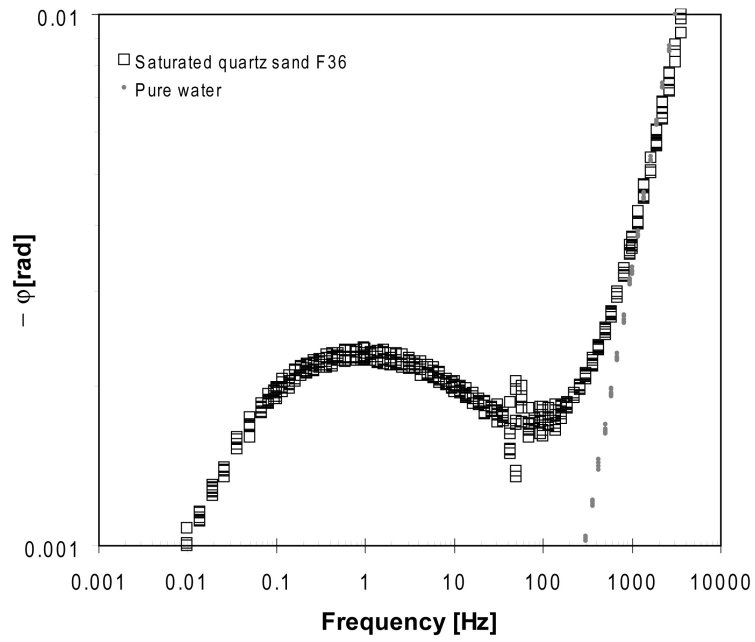


Fig. 2. Example of phase spectra obtained from SIP measurements on a saturated sample of sand F36 (Table 1) as well as on the corresponding saturating pore water alone. The latter had an electrical conductivity of $\sim 60 \mu\text{S/m}$. Note the negative scale for the phase.

6075

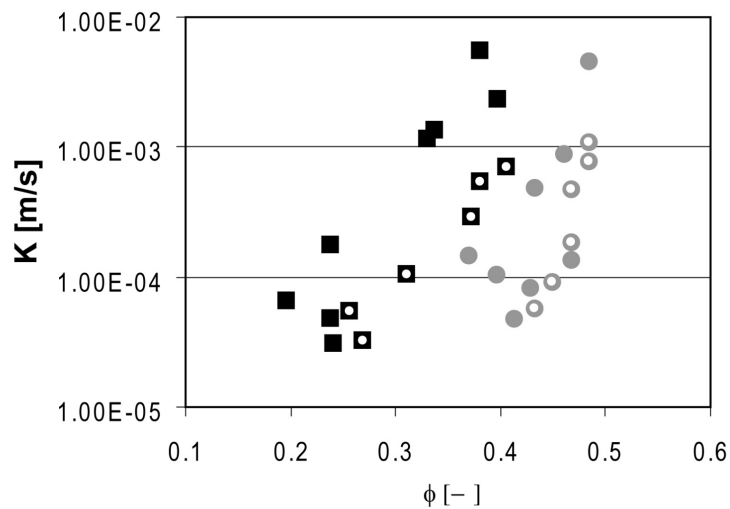


Fig. 3. Plot of the saturated hydraulic conductivity K versus porosity ϕ for all of the samples considered in this study. Black squares represent compacted, grey circles uncompact samples. White circles therein denote sieved, well sorted samples.

6076

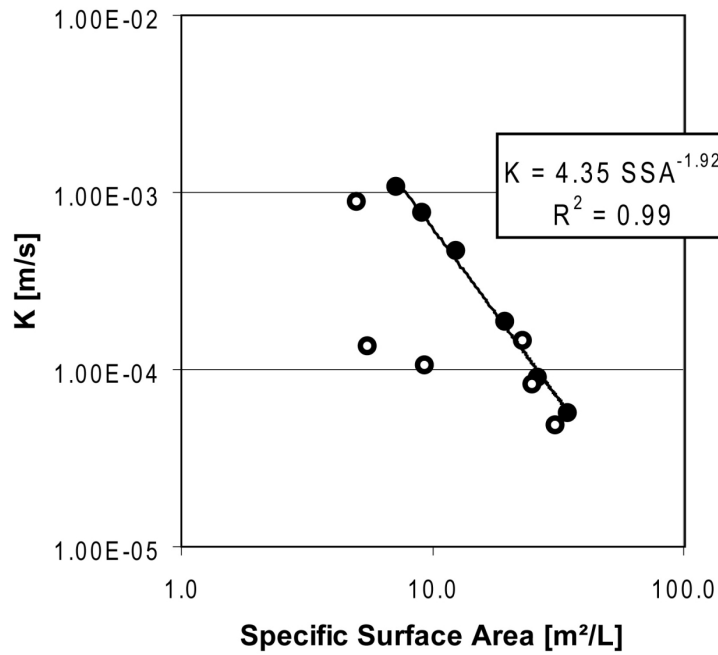


Fig. 4. Plot of the saturated hydraulic conductivity K versus specific surface area (SSA) for non-compacted samples having grain sizes smaller than 2 mm. Black solid circles denote sieved sand fractions, while non-solid circles represent unsieved samples.

6077

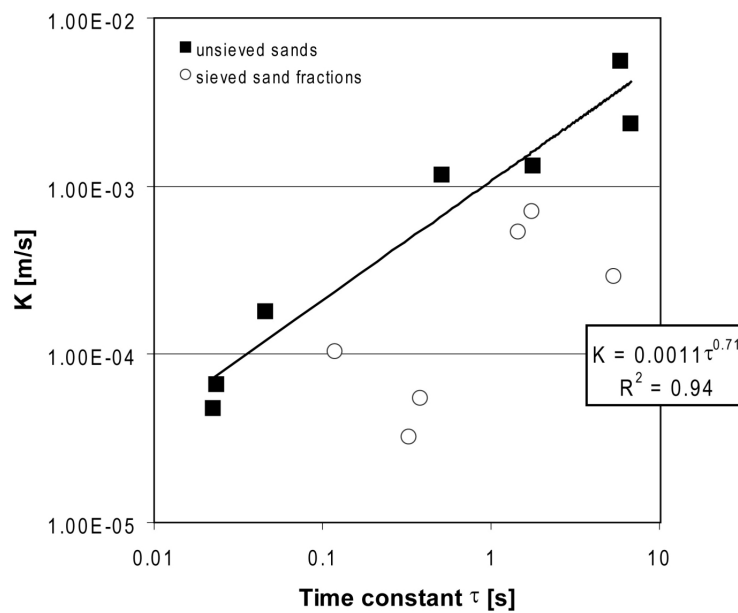


Fig. 5. Plot of the saturated hydraulic conductivity K versus Cole-Cole relaxation time τ for sieved and unsieved samples using a conductivity of $\sim 300 \mu\text{S/cm}$ for the saturating pore water. In both cases the samples were compacted.

6078

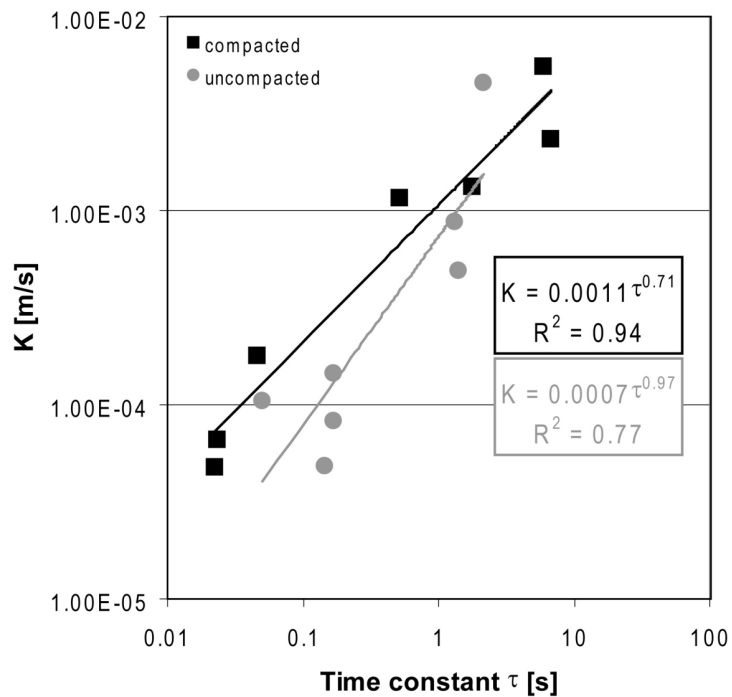


Fig. 6. Plot of the saturated hydraulic conductivity K versus Cole-Cole relaxation time τ for compacted and uncompact, both unsieved, samples measured at $\sim 300 \mu\text{S/cm}$ electrical conductivities of the saturating pore water.

6079

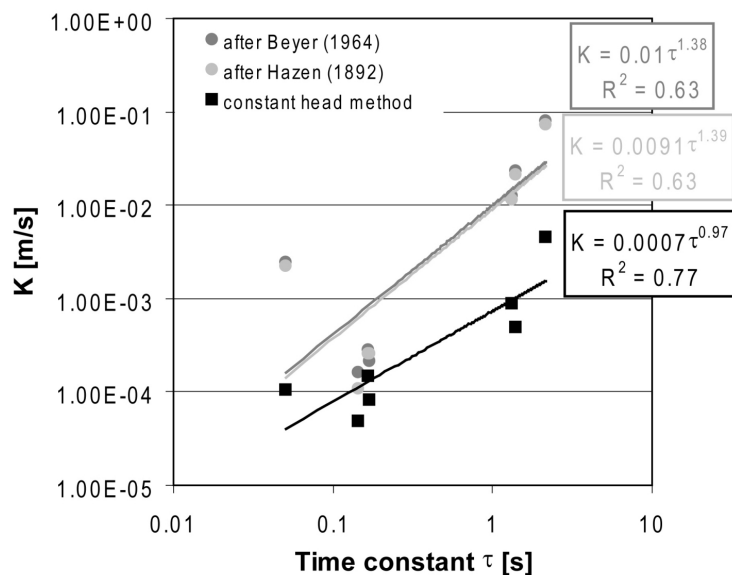


Fig. 7. Plot of the saturated hydraulic conductivity K versus the Cole-Cole relaxation time τ for uncompact samples measured at an electrical conductivity of the the saturating pore water of $\sim 60 \mu\text{S/cm}$. K either was calculated from the grain-size distribution measurements using the empirical, grain-size-based formulas of Beyer (1964) and Hazen (1892) or experimentally determined through constant-head-type measurements.

6080